The EMBO Journal (2010) 29, 532–545 | © 2010 European Molecular Biology Organization | All Rights Reserved 0261-4189/10
www.embojournal.org

THE EMBO JOURNAL

Identification of a novel Bves function: regulation of vesicular transport

Hillary A Hager[1], Ryan J Roberts[1], Emily E Cross[1], Véronique Proux-Gillardeaux[2] and David M Bader[1,*]

[1]The Stahlman Cardiovascular Research Laboratories, Program for Developmental Biology, and Department of Medicine, Vanderbilt University, Medical Center, Nashville, TN, USA and [2]Membrane Traffic in Neuronal and Epithelial Morphogenesis, Institut National de la Santé et de la Recherche Médicale ERL U950, Institut Jacques Monod, Unité Mixte de Recherche 7592, Centre National de la Recherche Scientifique, Université Denis Diderot Paris 7, Paris, France

Blood vessel/epicardial substance (Bves) is a transmembrane protein that influences cell adhesion and motility through unknown mechanisms. We have discovered that Bves directly interacts with VAMP3, a SNARE protein that facilitates vesicular transport and specifically recycles transferrin and β-1-integrin. Two independent assays document that cells expressing a mutated form of Bves are severely impaired in the recycling of these molecules, a phenotype consistent with disruption of VAMP3 function. Using Morpholino knockdown in *Xenopus laevis,* we demonstrate that elimination of Bves function specifically inhibits transferrin receptor recycling, and results in gastrulation defects previously reported with impaired integrin-dependent cell movements. Kymographic analysis of Bves-depleted primary and cultured cells reveals severe impairment of cell spreading and adhesion on fibronectin, indicative of disruption of integrin-mediated adhesion. Taken together, these data demonstrate that Bves interacts with VAMP3 and facilitates receptor recycling both *in vitro* and during early development. Thus, this study establishes a newly identified role for Bves in vesicular transport and reveals a novel, broadly applied mechanism governing SNARE protein function.

The EMBO Journal (2010) **29,** 532–545. doi:10.1038/emboj.2009.379; Published online 7 January 2010
Subject Categories: membranes & transport; development
Keywords: cellubrevin; integrin; Popdc; SNARE; *Xenopus*

Introduction

Vesicular transport is a conserved process where membrane-bound vesicles transfer material within the cell and to the cell surface. Protein trafficking and recycling through vesicles is crucial for a myriad of processes, including membrane-receptor localization and cell motility. Membrane trafficking consists of both endocytic and exocytic pathways that modulate receptors, ligands, and molecules that are present on the cell surface. While much is known about this process, identification of novel regulators is essential for a comprehensive understanding of the role vesicular transport plays in a broad spectrum of cell functions.

There are four essential steps of membrane trafficking: vesicle budding, transport, tethering, and fusion (Grosshans *et al*, 2006; Cai *et al*, 2007). Coat proteins and adaptor proteins select vesicle cargo and facilitate the initial step of vesicle budding (Cai *et al*, 2007; Mellman and Nelson, 2008). Rab GTPases and motor proteins primarily transport vesicles to the target membrane; however, there is accumulating evidence that Rab GTPases participate in every aspect of protein trafficking from budding to docking (Segev, 2001; Grosshans *et al*, 2006; Pfeffer, 2007). Vesicle tethering is performed by a diverse set of multi-subunit proteins (Grosshans *et al*, 2006). The final step in membrane trafficking is performed by SNARE proteins, which facilitate fusion of intracellular vesicles to the membrane (Brunger, 2005; Jahn and Scheller, 2006; Leabu, 2006). There are three families of SNARE proteins: vesicle-associated membrane proteins (VAMPs), membrane proteins located on the target membrane (syntaxins), and target-membrane-localized synaptosome-associated proteins (SNAPs) (Brunger, 2005; Jahn and Scheller, 2006; Leabu, 2006). These proteins interact to form a SNARE complex via their coiled-coil SNARE domains (Brunger, 2005; Leabu, 2006).

Vesicle-associated membrane protein-3 (VAMP3) is a ubiquitously expressed vesicular SNARE protein that binds syntaxin-4 in the basolateral region of epithelial cells to tether vesicular cargo to the membrane (Fields *et al*, 2007). VAMP3 recycles specific receptors to and from the plasma membrane through the recycling endosome (RE) (Galli *et al*, 1994; Breton *et al*, 2000; Polgar *et al*, 2002; Borisovska *et al*, 2005). VAMP3 has an established role in the recycling of transferrin and low-density lipoprotein receptor (LDLR), and is required for specific sorting through Adaptor Protein, 1B (McMahon *et al*, 1993; Fields *et al*, 2007). Disruption of VAMP3 results in aberrant localization of both transferrin and LDLR. Overall, VAMP3 is necessary for efficient transport of cargos, which subsequently act to mediate distinct cellular functions. Several studies have shown that VAMP3 is also required for cellular movement through trafficking of β-1-integrins. Disruption of VAMP3 results in reduced migration rate in wounded epithelial cells and slower cellular spreading on different substrates, as β-1-integrin recycling is impaired (Proux-Gillardeaux *et al*, 2005; Skalski and Coppolino, 2005; Tayeb *et al*, 2005; Luftman *et al*, 2009). Integrins stabilize lamellar protrusions through interactions with the ECM, and thus must be trafficked to the leading edge of the cell during migration (Caswell and Norman, 2006, 2008). In development, integrin-based cell motility is imperative for proper morphogenesis. This is evident in gastrulation of *Xenopus laevis*, where integrin adhesion to fibronectin (FN) underlies mesodermal migration and subsequent formation of the head and trunk (Ramos and DeSimone, 1996).

*Corresponding author. Department of Medicine, Vanderbilt University, 2220 Pierce Avenue, 348 PRB, Nashville, TN 37232, USA.
Tel.: +1 615 936 1976; Fax: +1 615 936 3527;
E-mail: david.bader@vanderbilt.edu

Received: 6 July 2009; accepted: 13 November 2009; published online: 7 January 2010

Blood vessel/epicardial substance (Bves) is a highly conserved member of the Popdc family of proteins (Hager and Bader, 2009). Bves exists as a dimerized three-pass transmembrane protein with an extracellular glycosylated N-terminus and an intracellular self-associating C-terminal tail (Knight *et al*, 2003; Kawaguchi *et al*, 2008). Within the C-terminus is the highly conserved Popeye domain, although no specific function has been linked to this motif (Brand, 2005; Osler *et al*, 2006). A wide variety of adherent tissues express Bves, including all three muscle types and various epithelia (Andree *et al*, 2000; Osler and Bader, 2004; Ripley *et al*, 2004; Vasavada *et al*, 2004; McCarthy, 2006; Osler *et al*, 2006; Smith and Bader, 2006; Torlopp *et al*, 2006). Bves localizes to the lateral region of the plasma membrane of epithelial cells, overlapping the distribution of junctional molecules such as E-cadherin, ZO-1, and occludin (Osler *et al*, 2005, 2006). In smooth, skeletal, and cardiac muscle Bves is observed around the circumference of cells (Smith *et al*, 2008). Intracellular punctate distribution is also observed in both polarized monolayers and unpolarized individual cells *in vitro*.

Disruption of Bves leads to a wide range of cell phenotypes in both vertebrates and invertebrates, the majority of which remain poorly understood at the molecular level. The trans-epithelial resistance of polarized epithelial cells is significantly decreased when Bves protein is knocked down, and junctional proteins such as E-cadherin, ZO-1, and β-catenin fail to traffic to points of cell–cell contact (Osler *et al*, 2005). Although Bves may play a role in localizing or stabilizing proteins at the membrane, the mechanism by which Bves functions in epithelial biogenesis remains completely unknown.

Most recently, Bves has been shown to interact with a Rho GEF, guanine nucleotide exchange factor-T (GEFT) (Smith *et al*, 2008). GEFT specifically activates Rac1 and Cdc42 to initiate filopodia and lamellipodia extension through rearrangement of the actin cortical network (Guo *et al*, 2003; Bryan *et al*, 2004, 2006). Disruption of Bves function results in increased cell roundness coupled with decreased activity of Rac1 and Cdc42, indicating decreased protrusion extension. Bves disruption also results in decreased cell movement, which is consistent with decreased Rac1 and Cdc42 activity (Smith *et al*, 2008). However, the exact mechanism by which Bves regulates GEFT remains unexplained.

Finally, Bves has been studied in the context of *X. laevis* gastrulation, where Bves is the only Popdc-family member expressed (Ripley *et al*, 2006; Hager and Bader, 2009). Frog gastrulation is highly dependent on cellular migration via integrin recycling (Ramos and DeSimone, 1996; Ramos *et al*, 1996; Marsden and DeSimone, 2001; Davidson *et al*, 2006), and protein knockdown suggests that Bves is necessary for cell movement (Ripley *et al*, 2006). Again, no prior data demonstrate the precise molecular and cellular mechanism underlying Bves function in *X. laevis*.

An emerging theme is that vesicular transport may underlie the essential biological processes in which Bves is involved: cell–cell adhesion, movement, and epithelial biogenesis. However, little is known about the mechanism by which Bves functions in these diverse yet fundamental processes. As inhibition of Bves function disrupts vital membrane functions and possibly vesicular transport, we conducted a split-ubiquitin screen to identify potential protein–protein interactions at the cell membrane. Here we report that Bves interacts with the SNARE protein, VAMP3, and that disruption or depletion of Bves results in impaired VAMP3-mediated vesicular transport. From these data, we hypothesize that Bves influences VAMP3 function to affect multiple cellular behaviours, and suggest that a role for Bves in the general process of vesicular transport may explain the varied nature of previously reported phenotypes.

Results

Bves interacts with VAMP3

Given the protein distribution of Bves, and previously reported phenotypes, we conducted a split-ubiquitin screen to detect Bves-interacting membrane proteins with characterized functions in cell movement (Dunnwald *et al*, 1999). VAMP3, a SNARE protein that facilitates the fusion of apposing membranes during vesicular transport (McMahon *et al*, 1993), was identified as a binding partner in this screen. Importantly, VAMP3 transports membrane proteins and is required for the vesicular transport underlying cell motility (Galli *et al*, 1994; Proux-Gillardeaux *et al*, 2005; Skalski and Coppolino, 2005; Tayeb *et al*, 2005). As Bves is also required for cell motility, and VAMP3 has a known function in this process, we chose to probe this interaction further.

To confirm this result, we determined whether Bves and VAMP3 proteins interact biochemically using co-immunoprecipitation (co-IP) and GST pull-down assays. As shown in Figure 1A, VAMP3 precipitated with Bves. Additionally, GST pull-down assays demonstrated a specific interaction between Bves and VAMP3, localized to the intracellular C-terminal Popeye domain (Figure 1B). Interestingly, Bves also interacts with VAMP2 via GST pull-down (Supplementary Figure 1). VAMP2 and VAMP3 are highly homologous, with only a one-amino-acid difference in their SNARE-binding domain (McMahon *et al*, 1993), suggesting conserved interaction between Bves and SNARE proteins.

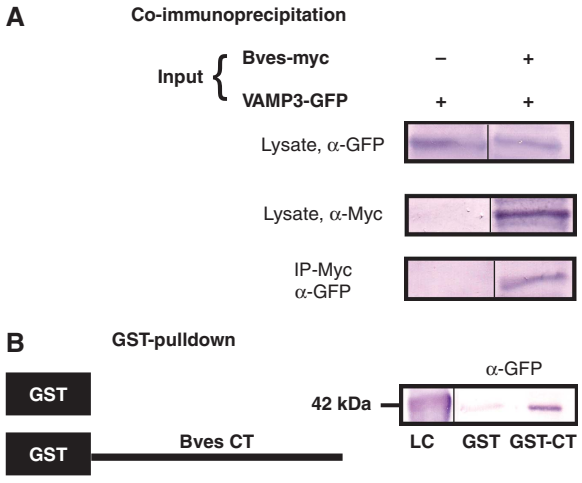

Figure 1 Bves and VAMP3 interact. For co-IP (**A**), COS-7 cells were transfected with tagged proteins, VAMP3–GFP alone or VAMP3–GFP and full-length Bves–myc. Cell lysates were pulled down with myc and blotted for GFP. In GST pull-down assays (**B**), the C-terminus of Bves was fused to GST (GST–CT) and was used to pull down transfected VAMP3–GFP from cell lysate. Loading controls (lysate in panel **A** and LC in panel **B**) are given.

Taken together, these data confirm the direct interaction of Bves with VAMP3 through its cytoplasmic tail.

Bves and VAMP3 colocalize

Bves and VAMP3 exhibit similar dynamic distributions that are both at the cell periphery and in intracellular compartments (Osler *et al*, 2005; Hager and Bader, 2009). Colocalization in Madin–Darby canine kidney (MDCK) cells of endogenous Bves (Figure 2A) and exogenously expressed VAMP3–GFP (Figure 2B) is readily observed both at the cell periphery and in intracellular vesicles (merge in Figure 2C, arrows). Although overlap is extensive, it is not complete, as some intracellular vesicles labelled with Bves are not co-labelled with VAMP3. Examining endogenous localization in confluent epithelial sheets, Bves (Figure 2D) and VAMP3 (Figure 2E) were seen colocalized in the lateral portion of MDCK cells and staining was also observed in intracellular vesicles (merge in Figure 2F, arrows). These data confirm that overlap of these two proteins is consistent with their previously reported endogenous distribution profile (Osler *et al*, 2005; Fields *et al*, 2007). Disruption of VAMP3 function (detailed below) resulted in significant decrease in the presence of Bves at the cell membrane (Supplementary Figure 2), while expression of a truncated Bves lacking the VAMP3-binding domain (also detailed below) produced only minor changes in protein distribution.

While VAMP3 is ubiquitously expressed across all non-neuronal tissue types, Bves is present at high levels in muscle as well as in other adherent or excitable tissues (McMahon *et al*, 1993; Hager and Bader, 2009). Thus, we characterized endogenous protein distribution in mouse heart and skeletal muscle to probe for colocalization. Significant colocalization was observed in both muscle types, although overlap was not absolute (Figure 3). Colocalization was seen primarily at the circumference of the myocytes, with certain muscle cells demonstrating more intense labelling (Figure 3C and G, white arrows). The intensity profiles (Figure 3D and H) of both Bves and VAMP3 signal demonstrate the high degree of colocalization (Figure 3C and G; red arrows indicate area of intensity profile). As Bves and VAMP3 both interact and colocalize, we next focused on functional assays to determine the potential importance of this interaction.

Transferrin recycling is attenuated in cells with disrupted Bves function

VAMP3 is required for recycling of transferrin, as cleavage of VAMP3 disrupts vesicular transport of this receptor (McMahon *et al*, 1993; Galli *et al*, 1994). To identify the potential role of Bves in VAMP3-dependent recycling, using a standard transferrin uptake assay, we developed an MDCK cell line that stably expresses only the first 118 amino acids of Bves (Bves118). Bves118 lacks the intracellular VAMP3-binding domain and contains only the short extracellular and transmembrane domains. Transferrin endocytosis was analysed at 5, 10, and 20 mins (Figure 4A) and mean fluorescence intensity (MFI) was analysed in MDCK and Bves118 cells. At 5-min internalization, average MFI (which directly correlates to the amount of endocytosed transferrin) for MDCK cells was 46.53, whereas Bves118 cells had an average MFI of 16.41, demonstrating decreased uptake of labelled transferrin. This trend continued at 10 and 20-min internalization with Bves118 cells having severely decreased internalization of labelled transferrin relative to MDCK cells (5 mins: $P<0.001$; 10 mins: $P<0.003$; 20 mins: $P<0.0036$). Disruption of transferrin kinetics was also demonstrated by a recycling assay, as labelled transferrin was exocytosed from Bves118 cells more slowly as compared with controls (Supplementary Figure 4). This phenotype is consistent with disrupted VAMP3 function and supports the hypothesis that Bves–VAMP3 interaction is necessary for VAMP3-mediated vesicular transport.

To corroborate and extend these studies with an *in vivo* model and directly compare the effects of transferrin recycling between Bves- and VAMP3-depleted embryos, we used a Morpholino (MO) knockdown and rescue strategy in *X. laevis* (Ripley *et al*, 2006). Embryos were injected with Bves MO, VAMP3 MO, or control MO (COMO); alternatively, sister embryos were co-injected with Bves MO or VAMP3 MO and their respective rescue RNAs (Bves MOR, VAMP3 MOR). Isolated animal caps, which express the transferrin receptor (NCBI, EST databases), were allowed to endocytose

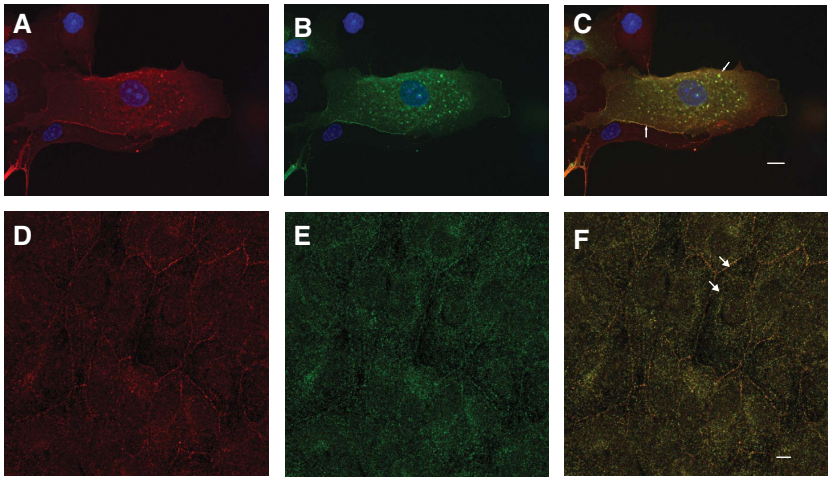

Figure 2 Bves and VAMP3 colocalize in MDCK cells. Both endogenous Bves (**A**) and transfected VAMP3–GFP (**B**) are observed at the membrane and in vesicles. The endogenous distribution of both proteins also demonstrates this same localization pattern (Bves, **D**; VAMP3, **E**), and Bves and VAMP3 colocalize in merged images (arrows, **C**, **F**). Scale bars are 5 μm.

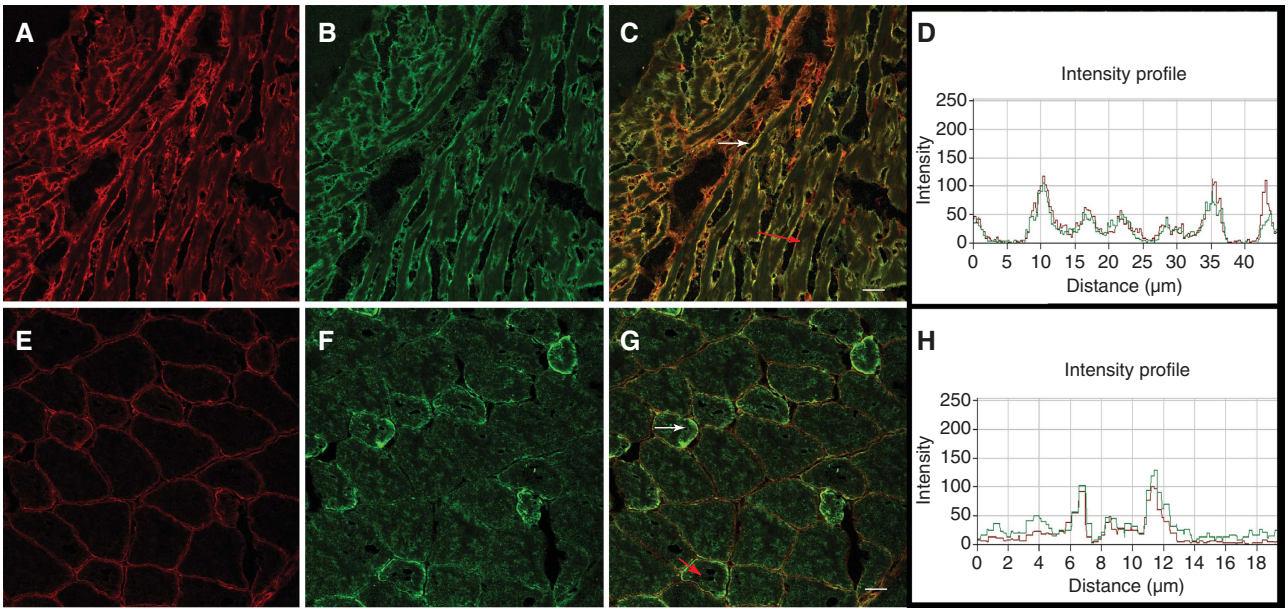

Figure 3 Endogenous Bves and VAMP3 colocalize in muscle. Bves (**A**, **E**) and VAMP3 (**B**, **F**) are seen at the cell periphery in adult cardiac (**A–C**) and skeletal muscle (**E–G**). Areas of intense colocalization are denoted by white arrows (**C**, **G**). Red arrows indicate the area of the fluorescent intensity profile for cardiac (**D**) and skeletal muscle (**H**). Scale bars are 20 μm.

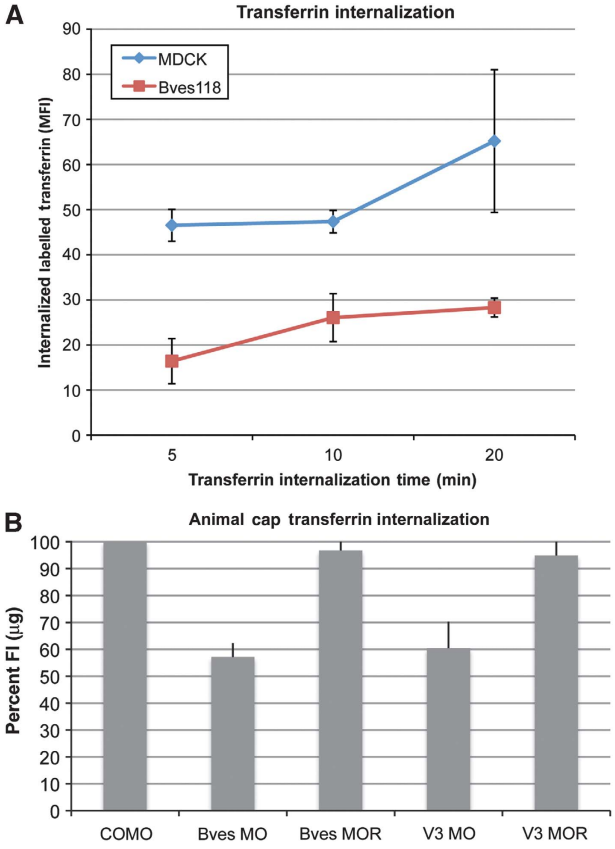

Figure 4 Transferrin uptake is attenuated when Bves is disrupted. (**A**) MDCK and Bves118 cells internalized labelled transferrin for 5, 10, or 20 mins. Transferrin uptake, as measured by the MFI, was significantly decreased in Bves118 cells at all time points. (**B**) When normalized with COMO values (100%), Bves MO- and VAMP3 (V3) MO-treated caps were impaired in internalization of labelled transferrin/μg of total protein. Transferrin uptake is restored when Bves MO or V3 MO are co-injected with rescue Bves (Bves MOR) or VAMP3 (V3 MOR) RNAs.

transferrin-633 for 25 mins and the fluorescent intensity (FI) per microgram of animal cap protein was determined. As shown in Figure 4B, recycling of labelled transferrin in Bves MO- and VAMP3 MO-treated animal caps is severely reduced relative to that in COMO-treated caps. When normalized against COMO-treated caps (100%), Bves MO-treated animal caps display only 57.2 ± 5.06% of FI/μg, demonstrating that recycling of labelled transferrin is inhibited when Bves is depleted (Table I). Similarly, VAMP3 MO-treated caps internalize 60.4 ± 9.9% of labelled transferrin relative to COMO (Table I). This reduction in recycling of labelled transferrin in animal caps is completely dependent on knockdown of Bves or VAMP3, as these phenotypes are rescued in caps co-injected with Bves rescue RNA along with Bves MO, or VAMP3 rescue RNA along with VAMP3 MO (Bves MOR: 96.8 ± 4.57% and VAMP3 MOR: 94.9 ± 12.14% of FI/μg relative to COMO-treated caps; Table I). Taken together, these two independent methods demonstrate that recycling of transferrin is attenuated after Bves disruption, suggesting that VAMP3-mediated transport is dependent on Bves function.

VAMP3-mediated recycling of β-1-integrin is impaired in cells expressing mutated Bves

VAMP3 function is necessary for recycling of β-1-integrin during cell movement (Proux-Gillardeaux *et al*, 2005; Skalski and Coppolino, 2005; Tayeb *et al*, 2005; Luftman *et al*, 2009). Proux-Gillardeaux *et al* have reported an *in vitro* scratch assay that directly tests VAMP3-mediated recycling of β-1-integrins by quantifying its recycling over time; we adapted this method by using β-1-integrin labelled with FITC. In wild-type (WT) MDCK cells, 59.6 ± 5% of cells at the free edge of the wound were positive for labelled integrin (Figure 5A–C and Table II). Bves118 cells showed dramatic decrease in endocytosed FITC-labelled integrins (Figure 5D–F). Note the limited number of Bves118 cells with

Table I Transferrin internalization in animal caps

COMO	Bves MO	Bves MOR	VAMP3 MO	VAMP3 MOR
% FI/μg of COMO				
100	57.2 ± 5.06	96.8 ± 4.57	60.4 ± 9.9	94.9 ± 12.14
	P-value	*P*-value	*P*-value	*P*-value
	< 0.0001	< 0.2111	< 0.0002	< 0.4340

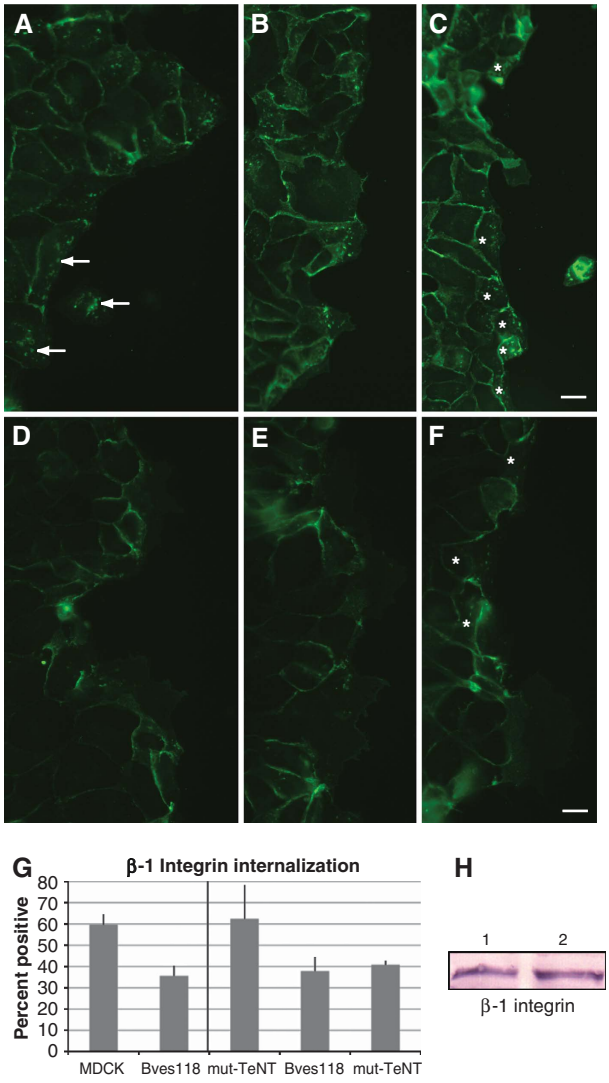

Figure 5 Cells stably expressing mutated Bves have decreased integrin recycling. A wounded monolayer of MDCK cells (**A–C**) internalized FITC-labelled β-1-integrin antibody (A, arrows, intracellular labelling) as cells migrated to close the wound. β-1-Integrin recycling is visualized by the presence of FITC-labelled protein in intracellular compartments. In Bves118 cells, integrin recycling was attenuated (**D–F**), as seen by decreased intracellular punctate labelling, although integrin expression levels of Bves118 (**H**, lane 2) cells are consistent with those in MDCK cells (**H**, lane 1). This decrease in integrin internalization is also seen when directly compared with that in WT-TeNT and mut-TeNT cells (**G**; Supplementary Figure 6). Cells marked by asterisk (**C**, **F**) were counted as integrin-positive (**G**; Table II). Scale bars are 20 μm.

internalized FITC-labelled integrin (35.5 ± 5%) as compared with WT MDCK cells (Figure 5G and Table II; $P < 0.0001$) even though β-1-integrin protein levels remain the same

Table II β-1 Integrin recycling

	MDCK	Bves118	
% Positive	59.6 ± 5	35.5 ± 5	
Total cells	1955	2597	
		P-value < 0.0001	
	mut-TeNT	Bves118	WT-TeNT
% Positive	62.4 ± 16	37.8 ± 7	40.8 ± 2
Total cells	733	768	816
		P-value < 0.004	*P*-value < 0.008

(Figure 5H). To confirm that disruption of Bves does in fact phenocopy the disruption of VAMP3, we repeated this assay using β-1-integrin antibody (CD29, clone Ha 2/5) conjugated to Alexa-564 and directly compared cells expressing WT tetanus toxin (WT-TeNT, which effectively cleaves VAMP3, rendering it unable to transport integrin) with Bves118 cells. Using the exact cell line in which disrupted integrin recycling upon VAMP3 knockdown was first reported (Proux-Gillardeaux *et al*, 2005), along with the control cell line that expresses mutant inactive tetanus neurotoxin (mut-TeNT), we determined in a side-by-side comparison that 37.8 ± 7% of Bves118 cells and 40.8 ± 2% WT-TeNT cells internalized labelled integrins, while 62.4 ± 16% of mut-TeNT cells were positive for integrin internalization (Figure 5G and Supplementary Figure 6). Additionally, internalized β-1-integrin colocalized with both Bves and VAMP3 antibodies (Supplementary Figure 5), supporting a role for Bves and VAMP3 in recycling of integrins. These data demonstrate that disruption of Bves and VAMP3 result in similar phenotypes and further support the hypothesis that intact Bves function is required for proper VAMP3-mediated recycling of different molecules.

Expression of mutated Bves or TeNT disrupts cell spreading

As Bves118 and WT-TeNT cells have impaired integrin uptake during cell movement, we determined whether another integrin-dependent function, cell spreading, was also disrupted. Cells were plated on FN at single-cell density and allowed to adhere for 45 mins prior to time-lapse analysis. At time 0, all four cell types, MDCK (Figure 6A), Bves118 (Figure 6C), mut-TeNT (Figure 6E), and WT-TeNT (Figure 6G), displayed similar areas and it was evident that cell protrusions were beginning to form. However, after 1 h of image acquisition, MDCK and mut-TeNT cells (Figure 6A and E, time 60) had greatly increased cellular areas (Figure 6J and Table III), 73 and 87% respectively, while Bves118 and WT-TeNT cells (Figure 6C and G; time 60) had cell areas increased only by 16 and 13%, respectively (Figure 6J and Table III). Time-lapse movies of all four cell types are given in Supplementary Figures 7–10. Kymographs of cell spreading over time reveal significant differences in cell spreading between MDCK (Figure 6B) and Bves118 cells (Figure 6D), as well as between mut-TeNT (Figure 6F) and WT-TeNT cells (Figure 6H and Table III). It should be noted that in a direct comparison of the area of cell spreading (Figure 6I), both experimental cell lines have similar areas of cell

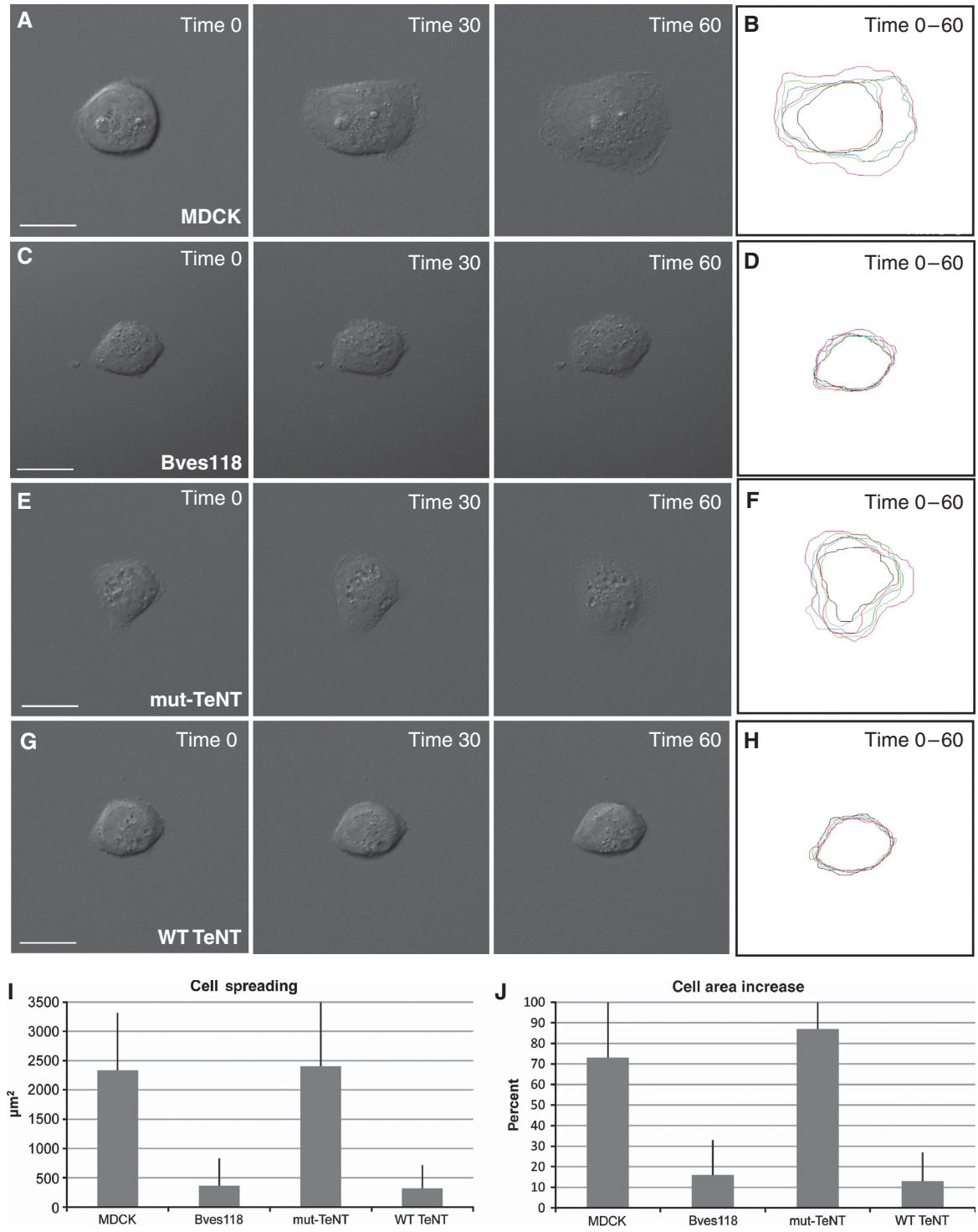

Figure 6 Cell spreading is attenuated with disruption of Bves or VAMP3 function. Time-lapse analysis indicates that cell spreading, or increase of area prior to polarized cell movement, is decreased in Bves118 cells (**C**) as compared with that in MDCK cells (**A**). Similarly, WT-TeNT (**G**) cells have less cell spreading than mut-TeNT cells (**E**). Kymographs of cell spreading demonstrate the difference in the degree of cell spreading between control and experimental groups (MDCK (**B**) vs Bves118 (**D**); and mut-TeNT (**F**) vs WT-TeNT (**H**)). Cell areas (**I**) and percent increase of cell area (**J**) for experimental groups and control groups as determined from composite kymographs are given (**B**, **D**, **F**, **H**). Scale bars are 20 μm.

spreading (Bves: 363 μm^2 and VAMP3: 318 μm^2), which are significantly reduced from the areas observed in both control cell lines (MDCK: 2337 μm^2 and mut-TeNT: 2401 μm^2). Individual frames of composite kymographs shown in Figure 6B, D, F, and H are given in Supplementary Figure 11. These data, which are corroborated using the *X. laevis* system (see below), demonstrate that cell spreading is significantly impaired in cells with mutated Bves or VAMP3, suggesting that interaction of these two proteins is important for integrin-mediated processes.

Table III MDCK cell spreading quantification

	MDCK	Bves118	mut-TeNT	WT-TeNT
% Area increase	73 ± 30	16 ± 17	87 ± 49	13 ± 14
P-value <		0.0001		0.0007
Cell spreading (μm^2)	2337 ± 979	363 ± 466	2401 ± 1111	318 ± 396
P-value		0.0001		0.0002

Morphological defects are observed in Bves- and VAMP3-depleted X. laevis embryos

Having established that Bves is required for VAMP3-mediated vesicular transport *in vitro*, we next determined the *in vivo* significance of this interaction. Gastrulating *X. laevis* embryos undergo extensive integrin-dependent cellular rearrangement, hence this is an advantageous system in which to analyse Bves function in development (Keller, 1980; DeSimone *et al*, 2005). Bves-depleted embryos (via aforementioned MO knockdown) exhibited delayed closure of the blastopore during gastrulation, which is indicative of disrupted cellular movement (Figure 7B) (Johnson *et al*, 1993; Ramos and DeSimone, 1996; Ramos *et al*, 1996; Marsden and DeSimone, 2001, 2003). Similarly, embryos injected with VAMP3 MO displayed a delay in blastopore closure (Supplementary Figure 12B), although this phenotype was less penetrant when compared with the Bves phenotype. It is interesting that similar defects are seen at this stage, as this is when integrin-mediated adhesion is important for migration across the blastocoel roof (BCR), which results in blastopore closure (Marsden and DeSimone, 2001). The BCR intercalates to become two-to-three cell layers thick in COMO-injected embryos (Figure 7D, arrow), but remained thickened in Bves-depleted embryos upon histological analysis (Figure 7E, arrow; Keller, 1980). Additionally, the involuting mesoderm is disassociated from the BCR in Bves-depleted embryos, suggesting decreased cell–matrix adhesion (Figure 7E, asterisk). Interestingly, *X. laevis* embryos injected in one of two cells with a lower dose of Bves MO (20 ng) display anterior defects characterized by disrupted morphogenesis of head structures and ectodermal outgrowths on the injected side (Figure 7C, arrows). These phenotypes are completely dependent on inhibition of Bves function, as total rescue is achieved by co-injecting Bves MO with 100 pg of *X. laevis* Bves mRNA (Supplementary Figure 13). Conversely, VAMP3 MO-treated embryos did not display overt defects in the anterior region at the tadpole stage and generally had a less severe phenotype compared with Bves MO-treated embryos, which was characterized by a shorter anterior–posterior (AP) axis and moderate-to-severe oedema (Supplementary Figure 12).

In *X. laevis*, anterior structures are the progeny of the involuting head mesoderm (HM); thus, we further analysed this population of cells (region denoted by asterisk in Figure 7E; Kumano and Smith, 2002). Involuting HM uses integrin adhesion to migrate along an FN gradient that is distributed on the BCR (Smith *et al*, 1990). These cells are directionally polarized towards the leading edge and extend lamellipodia (Winklbauer and Nagel, 1991). Scanning electron microscopy (SEM) and quantitative morphometrics of this region revealed significant changes in cell polarity and overlap in experimental embryos when compared with controls (Table IV). SEM of Bves-depleted embryos showed that the anterior population of HM was severely disorganized (Figure 7H and J), with fewer overlaps, large spaces between cells, and no detectable polarity of cell orientation (Figure 7H and J, and Table IV). In contrast, control embryos displayed a 'shingle-like' pattern of overlapping cells that are all situated in a similar direction relative to the leading edge of the involuting mesoderm (Figure 7G and I; Winklbauer and Nagel, 1991). Taken together, these data suggest that gastrulation movements have been disrupted in both Bves MO- and VAMP3 MO-treated embryos, and that Bves function is necessary for proper orientation, cell contact, and morphology of HM during involution. Previous studies show that inhibition of integrin function results in overt defects in cellular movement, similar to those seen in Bves-depleted embryos (Figure 7; Ramos and DeSimone, 1996; Marsden and DeSimone, 2001; Na *et al*, 2003).

Bves-depletion results in decreased X. laevis cell spreading on FN

Integrins are required for migration of the involuting HM over an FN gradient during gastrulation of *X. laevis* (Marsden and DeSimone, 2001). As integrins are recycled by VAMP3, we next determined whether this was potentially an integrin-dependent phenotype (Proux-Gillardeaux *et al*, 2005; Skalski and Coppolino, 2005; Tayeb *et al*, 2005; Luftman *et al*, 2009). By plating primary disassociated HM cells on FN, we found that COMO cells had defined lamellipodia and displayed spread morphology *in vitro* (Figure 8A), as defined by previous published studies (Ramos and DeSimone, 1996). Conversely, Bves-depleted cells exhibited distinctly decreased cellular spreading on FN (Figure 8B), with smaller cell protrusions. Previous reports have demonstrated disruption of integrin function results in round or spherical cells, phenocopying Bves depletion (Ramos and DeSimone, 1996). This decrease in spread morphology was not due to decrease in integrin expression levels, as Bves MO-injected embryos expressed the same level of integrin protein as COMO-treated embryos (Figure 7F). The majority of Bves-depleted cells remain rounded (79.2 ± 6%), with few filopodia anchoring them to FN (Figure 8B, arrows, and Table Va). Conversely, 73.6 ± 4% of control cells were spread in morphology. This result was significant, with $P < 0.0002$.

We next used live-cell imaging to determine whether Bves-depleted cells displayed impaired cell spreading, morphology, or movement over time; additionally, we extended this study to examine the effect of VAMP3 MO on HM-cell morphology. HM cells injected with COMO, Bves MO, or VAMP3 MO displaying spread morphologies were chosen at the onset of image capture and were visualized by previously co-injected membrane GFP (mGFP, experimental) or RFP (mRFP, control) (Wallingford *et al*, 2000). The behaviour of individual cells was recorded over time and subjected to kymographic analysis for cell spreading and morphology. Both control and experimental cells display a heavily yolk-laden appearance (Figure 8C, E, and G, and Supplementary Figures 14–17) and no cell in any group exhibited 'directional' migration over the course of study. Time-lapse analysis demonstrated COMO-injected cells (Figure 8C and Supplementary Figure 14) to display on average 4.45 ± 2.3 lamellipodia per cell, while Bves or VAMP3 MO-treated cells had only 0.98 ± 1.5

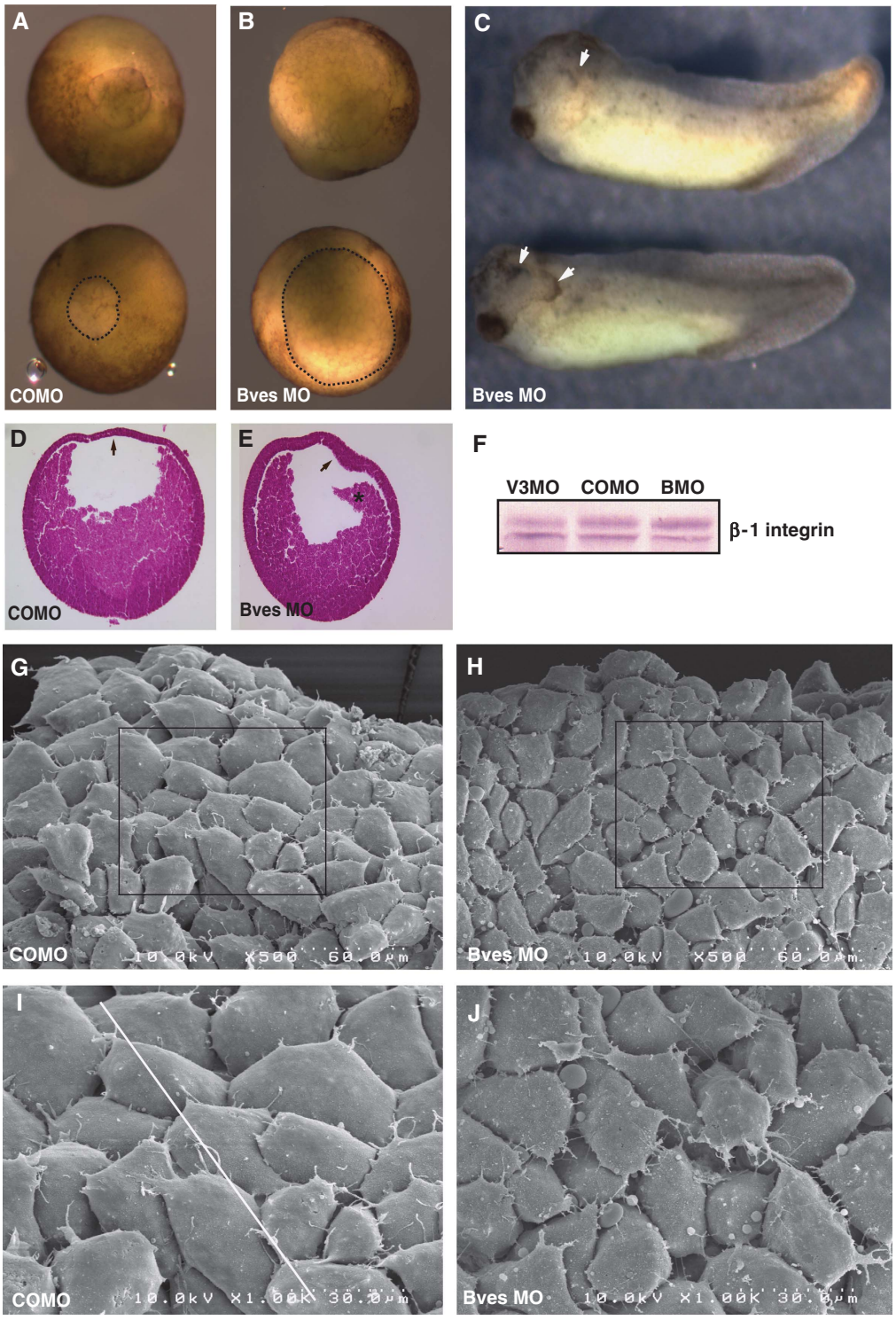

Figure 7 Bves depletion in *X. laevis* embryos. Blastopore closure in embryos injected with Bves MO was decreased (**B**) in comparison to embryos injected with COMO (**A**). The blastopore is outlined in the bottom embryo in panels A and B for better visualization. Anterior defects are observed in Bves-depleted, stage-35 embryos (**C**), characterized by disrupted eye morphogenesis and ectodermal outgrowths (arrows). Histological staining demonstrates the BCR remains thickened (**E**, arrow), whereas the BCR of control embryos has thinned (**D**, arrow). Also, the involuting HM has become detached from the BCR in Bves-depleted embryos (**E**, asterisk). Integrin levels in Bves MO- or VAMP3 MO-treated embryos are similar to those in COMO-treated embryos (**F**). In SEM analysis of HM, COMO-injected embryos display a distinct pattern of overlapped and polarized cells (**G**, **I**, white line indicates direction of polarity), whereas Bves MO-injected embryos lack directionality, have increased spaces between cells, and exhibit irregular cell shapes (**H**, **J**; quantified in Table IV). Panels **I** and **J** show magnified views of the boxed areas in panels **G** and **H**, respectively.

and 1.7 ± 1.7 lamellipodia/cell (Figure 8J and Table Vb). As previously reported (Ramos and DeSimone, 1996), when integrins are non-functional, cultured HM cells remain round in appearance. This was clearly observed in both Bves- and VAMP3-depleted cells (Figure 8E and G and Supplementary Figures 15 and 16). In a controlled side-by-side comparison of

Table IV SEM quantification

	Total cells	Overlaps/cell
Cell overlap		
COMO	67	1.66 ± 0.42
Bves MO	64	0.641 ± 0.41
	COMO	Bves MO
Cell polarity		
σ Avg	12.5 ± 3.7	50.2 ± 9.0

cells plated on the same FN-coated dish, Bves-depleted cells (labelled with mGFP) became rounded over time while COMO-treated cells (labelled with mRFP) remained spread (Supplementary Figure 17). Additionally, both Bves- and VAMP3-depleted cells often exhibited large and very transient bleb-like protrusions that harboured yolk granules (Figure 8E and G, arrows); in control cells (Figure 8C), yolk granules indicate the stable boundary between the cell body and cell protrusion (Selchow and Winklbauer, 1997). These membrane blebs, known as circus movements, in early development (Johnson, 1976) were short-lived and are generally thought to be associated with decreased adhesion or breakdown of the actin-cytoskeleton network (Shook and Keller, 2003; Fackler and Grosse, 2008). Kymographs of the area of attachment reveal that Bves- and VAMP3-depleted cells had a significantly smaller area of interaction with the substrate (Figure 8D, F, H, and K; see Supplementary Figure 18 for individual frames) when compared with COMO-injected cells. These statistically significant results (Table Vc) demonstrate that cell adhesion and process extension, processes regulated by integrins (Holly *et al*, 2000; Caswell and Norman, 2006), are impaired in Bves- and VAMP3-depleted cells. These data, which are corroborated by our current findings with MDCK cells, further support a role for Bves in cell movement through VAMP3-mediated recycling of integrins.

Discussion

In this study we present data that link Bves to the fundamental cellular process of vesicular transport. Bves has been previously reported to regulate cell movement and cell–cell adhesion, although these functions were unexplained at the molecular level. Here we describe a mechanism that may elucidate the role Bves plays in these processes through its interaction with the vesicular transport protein, VAMP3. Our findings demonstrate that the intracellular domain of Bves interacts directly with VAMP3, and that these proteins colocalize in a variety of cell types. Furthermore, stable expression of a mutant form of Bves or elimination of Bves protein function results in similar disruption in transport of two independent molecules, transferrin and β-1-integrin, both of which are trafficked by VAMP3 (Galli *et al*, 1994; Proux-Gillardeaux *et al*, 2005). These findings are corroborated in *X. laevis* embryos, where Bves depletion (as well as depletion of VAMP3) results in impaired transferrin recycling in animal caps and morphological defects consistent with the disruption of integrins. Furthermore, in both model systems, cells with inhibited Bves function have disrupted cell adhesion or spreading, consistent with VAMP3-dependent trafficking of integrins. Based on these data, we propose that Bves is essential for VAMP3 function in vesicular transport, and is specifically required for recycling of VAMP3-mediated receptors. Thus, we propose that Bves functions in broad cellular processes regulated by vesicular transport, explaining previously reported phenotypes unresolved at the molecular level.

Bves as a novel regulator of vesicular transport

Bves is essential for proper cell movement, although the exact role Bves played in this process was previously unknown (Ripley *et al*, 2006; Smith *et al*, 2008). We propose that, through interaction with VAMP3, Bves is necessary for vesicular transport of the adhesion molecule, β-1-integrin, as attenuated integrin recycling is observed during cell migration when Bves is disrupted. This retardation in integrin recycling exactly phenocopies VAMP3 disruption and directly links Bves disruption to impaired integrin recycling. These data are corroborated by attenuated cell spreading or adhesion (processes dependent upon integrin integrity) observed with Bves inhibition. Furthermore, impaired recycling of integrins is a potential mechanism explaining the gastrulation phenotype observed in the embryo.

VAMP3 transports transferrin; hence, the rate of transferrin uptake is a general indicator of the integrity of VAMP3 trafficking (Galli *et al*, 1994). With Bves disruption, either by expression of a mutated protein or protein depletion, endocytosis of transferrin decreases over time and phenocopies VAMP3 inhibition. These data, along with decreased recycling of β-1-integrin, demonstrate that Bves is important for VAMP3-mediated vesicular transport of receptors.

Bves is important for generation and maintenance of epithelial junction integrity (Osler *et al*, 2005). In the process of epithelial biogenesis, cell–cell adhesion is initiated as specific proteins are trafficked to the forming adherens junctions (Bryant and Stow, 2004; Yap *et al*, 2007). This process is disrupted upon Bves depletion, as the canonical adherens junction molecule, E-cadherin, is not localized to points of cell–cell contact (Osler *et al*, 2005). Cadherin-based cell adhesion is a dynamic process, with E-cadherin constantly being replenished at the cell surface via vesicular transport (Bryant and Stow, 2004; Yap *et al*, 2007). Defects in vesicular transport of E-cadherin could lead to disrupted cell adhesion or signalling, which results in pathogenic states such as metastatic cancer (Hirohashi, 1998). Recently, it has been shown that efficient delivery of E-cadherin is dependent on functional Rab11-positive REs (Desclozeaux *et al*, 2008). Disruption of either Rab11 (a Rab GTPase and a known candidate in vesicular transport) or the RE results in apical delivery of proteins. VAMP3 is a well-known member of the RE (Skalski and Coppolino, 2005; Fields *et al*, 2007) and thus it is plausible to hypothesize that VAMP3-mediated vesicle fusion may be important for recycling of E-cadherin, and mislocalization of E-cadherin upon Bves depletion may be explained by disrupted VAMP3-mediated vesicular transport. Thus, the current data and previous results suggest that Bves may influence vesicular transport in a broad array of cell functions.

Bves in cell adhesion, spreading, and movement

We provide conclusive evidence that Bves-depleted embryos have disrupted cell movements during gastrulation. *X. laevis*

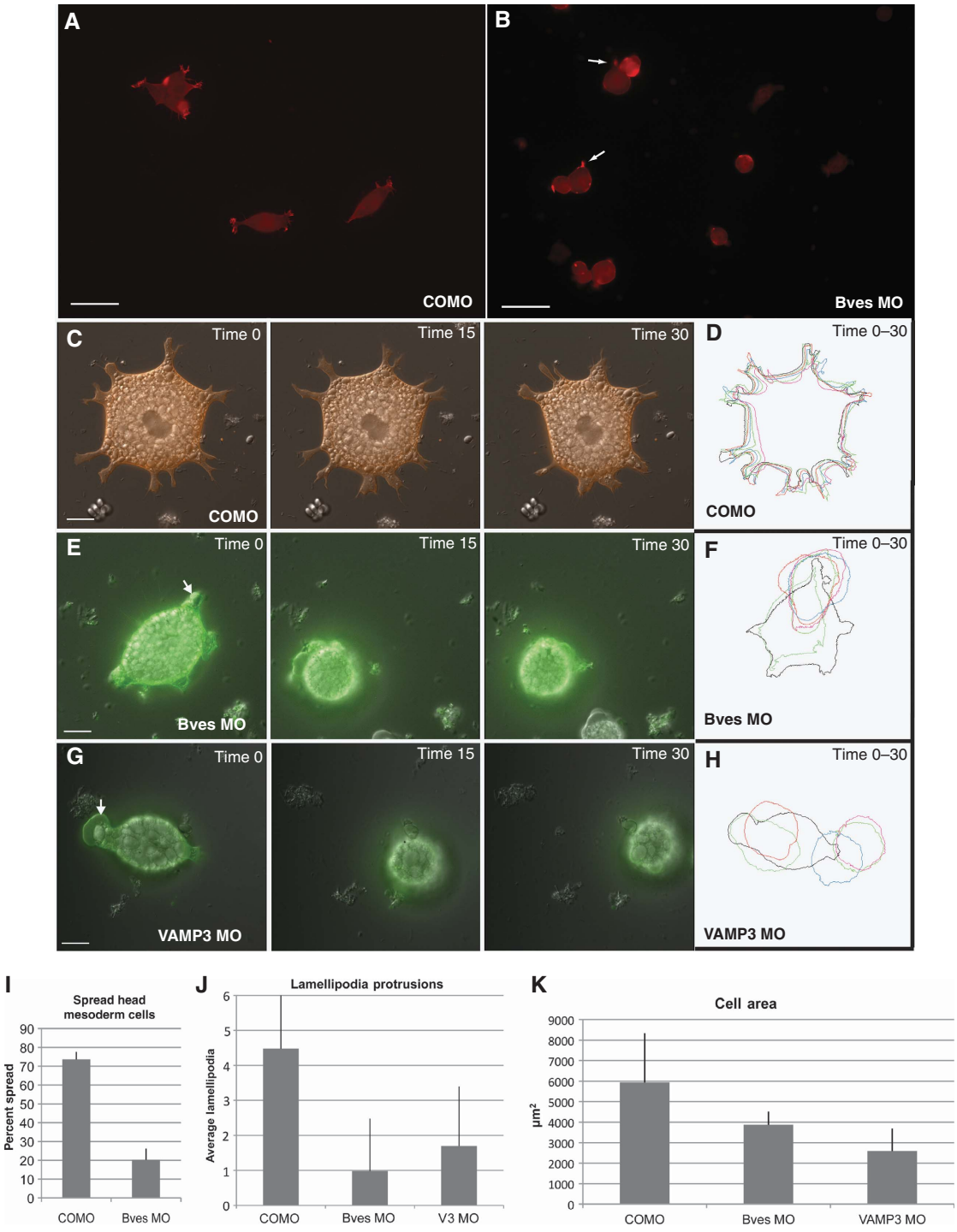

Figure 8 Bves- and VAMP3-depleted cells display decreased cell adhesion on FN. HM cells stained with phalloidin-568 from COMO-injected embryos (**A**) display spread morphologies on FN, while Bves-depleted cells (**B**) are round. Analysis over time (in minutes) indicates that as an mRFP-labelled, COMO-treated cell moves (**C**, time 0–30) it maintains a spread phenotype, extending several lamellipodia. Conversely, mGFP-labelled, Bves (**E**, time 0–30) or VAMP3 (**G**, Time 0–30)-depleted cells become rounded. Kymographs (**D**, **F**, **H**) depict cell morphology over time, demonstrating the differences in cell shape, lamellipodia number, and cell area, which are quantified in graphs in panels **I**, **J**, and **K**. Scale bars are 100 μm (**A**, **B**) and 20 μm (**C**, **E**, and **G**).

gastrulation is a well-studied system where integrin-dependent cell adhesion and movement are critical for development (Marsden and DeSimone, 2003; Davidson *et al*, 2006). We report that HM cells in Bves-depleted embryos fail to orient properly and, when isolated, display rounded morphology and impaired process extension when plated on FN. Additionally, these cells display transient membrane blebs, which have been associated with decreased cell adhesion during development (Shook and Keller, 2003), and indicate localized breakdown of the actin-cytoskeletal network (Fackler and Grosse, 2008). Evidence of this breakdown is seen in Bves-depleted cells as yolk granules, which are

Table V Head mesoderm cell adhesion quantification

	COMO	Bves MO	
(a) Cell spreading			
% Spread	73.6 ± 4	20.2 ± 6	
% Round	26.4 ± 4	79.2 ± 6	
Total cells	557	414	
P-value <		0.0002	
	COMO	Bves MO	VAMP3 MO
(b) Lamellipodia formation			
Lamellipodia/cell	4.45 ± 2.3	0.98 ± 1.5	1.7 ± 1.7
P-value <		0.0001	0.0001
	COMO	Bves MO	VAMP3 MO
(c) Cell area (μm^2)			
	5941 ± 2401	3872 ± 644	2592 ± 1097
P-value <		0.046	0.001

usually confined to the cell body, extend into lamellipodia (Selchow and Winklbauer, 1997). The decreased integrin-mediated cell–substrate adhesion, coupled with actin-cytoskeletal network breakdown found in these cells, is not surprising. Bves depletion influences Rac and Cdc42 activity (Smith *et al*, 2008), both of which are molecules that are important for actin polymerization and communicate with integrins during cell movement (DeMali *et al*, 2003). Additionally, actin polymerization has a well-documented role in the endocytic pathway (Lanzetti, 2007). Overall, these gastrulation-stage phenotypes are consistent with disrupted integrin function, as integrins are responsible for cell adhesion and spreading on FN (Marsden and DeSimone, 2001). As VAMP3 is known to recycle integrins, our data suggest VAMP3 interaction with Bves is necessary for proper integrin-dependent movements during early *X. laevis* development.

In turn, several previous reports have linked Bves to regulation of cell movement. For example, germ-cell migration in the developing *Drosophila* embryo is impaired with mutation of *Dmbves* (Lin *et al*, 2007), while Bves/Popdc1-null mice exhibit impaired skeletal muscle regeneration due to inhibition of myoblast movement (Andree *et al*, 2002). Previous work of our own group has demonstrated impaired movement and regulation of cell shape *in vitro* and in development (Ripley *et al*, 2004, 2006; Smith *et al*, 2008). Still, until identification of Bves–VAMP3 interaction, the mechanism underlying these phenotypes was unresolved. Interestingly, the *Bves* gene is hypermethylated in specific cancer types (Feng *et al*, 2008), suggesting gene silencing may coincide with downregulation of cell–cell adhesion. Thus, the role of Bves in the modulation of SNARE function may have broad impact on development and disease.

Bves as a moderator of diverse cellular pathways

In addition to interacting with VAMP3, we show that Bves interacts with VAMP2. It has been reported that VAMP2 and VAMP3 are promiscuous during development and *in vitro*, substituting for each other when one molecule is absent (Bhattacharya *et al*, 2002; Deak *et al*, 2006). This comes as no surprise, as rat VAMP2 and VAMP3 are highly homologous, differing by only one amino acid in their SNARE-binding domain (McMahon *et al*, 1993). Bves interaction with VAMP2, and the potential overlapping function between different VAMP homologues, may explain the milder phenotype observed in VAMP3-depleted *X. laevis* embryos, and may suggest a broader role for Bves in influencing VAMP-mediated vesicular transport. Additionally, VAMP2 is expressed in muscle satellite cells and is upregulated during skeletal muscle regeneration (Tajika *et al*, 2007); interestingly, this process is delayed in Bves-knockout mice (Andree *et al*, 2002). Finally, Bves is highly expressed in the brain, tissue where VAMP1 and VAMP2 are also enriched, although Bves has never been studied in this context (Hager and Bader, 2009). It would be interesting to determine whether Bves interacts with VAMP1, and whether interaction with VAMP1 or VAMP2 had any functional significance in the nervous system. Overall, Bves interaction with VAMP2 may suggest a broader role for Bves in a variety of tissue types that utilize SNARE machinery.

Current and recent studies have shown that Bves interacts with two proteins, VAMP3 and GEFT, that function through downstream targets to regulate convergent cellular processes (Smith *et al*, 2008). In light of the present data, it is intriguing to consider the overlapping cell operations in which VAMP3 and GEFT are involved, and how Bves interaction with either protein contributes to the phenotypes observed upon Bves disruption. Although direct functions of VAMP3 and GEFT within the cell are very different, they are nonetheless involved in common pathways. GEFT activates Rho GTPases, which in turn regulate cell adhesion, cell motility, polarity, gene expression, and membrane trafficking (Etienne-Manneville and Hall, 2002). VAMP3, through regulation of protein trafficking, modulates cell motility, polarity, and gene expression (Schwartz and Shattil, 2000). Indeed, several studies have even implicated Rho GTPase activity in the regulation of vesicular transport (Ridley, 2001; Symons and Rusk, 2003), and integrins have been shown to recruit Rho GTPases necessary for modulation of the actin network (Holly *et al*, 2000; Caswell and Norman, 2008). However, the interplay between integrin signalling and Rho GTPase function is not entirely understood. We hypothesize that through interaction with VAMP3 and GEFT, Bves may provide cross-talk to achieve cellular synchrony in these essential cell processes, and that the phenotypes observed upon Bves depletion in the current study may be in part due to disruption of Bves interaction with GEFT. It is likely that Bves regulates both pathways downstream of VAMP3 and GEFT simultaneously; however, the contribution of each pathway to cell adhesion and morphology remains to be determined. Thus, we propose that Bves is imperative for tight regulation of membrane dynamics in cell adhesion and movement through modulation of multiple signalling pathways. Taken together, our data suggest that Bves may play an unexpected role in a broad spectrum of cellular functions regulated by vesicular transport.

Materials and methods

For all assays described below, data were analysed with Microsoft Excel and error bars indicate standard deviation (s.d.); Student's *t*-tests were standard.

Antibodies, constructs, cell lines, tissue processing, and protein harvest

VAMP3–GFP and VAMP2–GFP were generous gifts from Dr W Trimble (University of Toronto) (Bajno *et al*, 2000). Rescue RNA that is mutated in the MO-binding site was used for *X. laevis* experiments as reported (Ripley *et al*, 2006). Rat VAMP3 was cloned into pCMV-3tag-4A and RNA was synthesized with mMESSAGE mMACHINE (Ambion). Bves antibodies SB1 and B846 were reported by Wada *et al* (2001) and Smith and Bader (2006). All other antibodies and reagents were obtained commercially as follows: anti-VAMP3 (Novus Biologicals, NB300-510, and Santa Cruz Biotechnology, sc-18208, clone N-12); anti-β-1-FITC (BD Pharmingen, clone Ha 2/5 555005); anti-CD29 (BD Transduction Laboratories, clone 18, 610468); anti-CD29 (BD Transduction Laboratories, clone Ha 2/5, 555003); anti-8C8 supernatant (*X. laevis* β-1-integrin) (Developmental Studies Hybridoma Bank); anti-GFP (Clonetech, JL8); anti-myc (Sigma, M4439 and C3956); anti-GST (GE Healthcare); and phalloidin-488 and 568 (Molecular Probes). MDCK cells were obtained from ATCC. Tissue processing and western blotting followed standard protocols (Ripley *et al*, 2006).

Split-ubiquitin screen

A split-ubiquitin screen was conducted by Dualsystems (Zurich, Switzerland). Full-length mouse Bves was cloned into pCCW-Ste and screened against a mouse adult heart library cloned into pDSL-Nx. VAMP3 passed all selection tests.

GST pull down and co-IP

Lysates were prepared as follows: COS-7 cells were transfected with either VAMP3–GFP alone or both VAMP3–GFP and Bves–myc, and confluent monolayers were harvested by rocking at 4°C for 1 h in CHAPS buffer (50 mM Tris–HCl (pH 8.0), 150 mM NaCl, 10 mM EDTA, 1% CHAPS) plus protease inhibitors (Roche, 11697498001). Lysates were collected and spun down at 18 000 *g* for 30 mins at 4°C. Co-IPs were conducted using protein-G Magnetic Dynabeads and a Dynal MPC Magnet as per manufacturer's instructions (Invitrogen). Bves–GST pull downs of VAMP–GFP proteins were conducted as previously published (Smith *et al*, 2008); western blots were standard.

Generation of stable cell lines

The extracellular and transmembrane domains of mouse Bves (amino acids 1–118; referred to as Bves118) were cloned in frame into pCMV-3myc-4A (Stratagene). Bves118 was nucleofected into MDCK cells according to the manufacturer's specifications (Amaxa). Three individual clones were selected and maintained in 400 μg/ml of G418. RT–PCR and immunofluorescence confirmed the expression of stably transfected tagged proteins (Supplementary Figure 3). Cell lines expressing WT-TeNT or mut-TeNT have been described by Proux-Gillardeaux *et al* (2005).

Transferrin assays

MDCK cells. Uptake of Alexa-633- or Alexa-488-labelled transferrin (Invitrogen, T23362, T13342) was assessed by flow cytometry. Briefly, cells that had been passaged three times were incubated in DMEM and 0.2% BSA for 2 h at 37°C and then incubated for 30 mins with 50 μg/ml of labelled transferrin at 4°C in the dark. Cells were allowed to internalize labelled transferrin at 37°C for the indicated time periods and then washed 4 × with ice-cold PBS on ice. Cells were probed for MFI using a BD FACS Canto II; data were acquired with Diva 6.0, analysed with WinList, and are reported as the average MFI from four different experiments.

Animal caps. Internalization of labelled transferrin-633 (Invitrogen, T23362) in animal caps was measured using a T-format spectrofluorometer (PTI Quantamaster 2000-7SE). Animal caps were dissected at stage 9–10 in 1 × Modified Barth's saline (MBS) and 0.1% BSA and then serum-starved in agar-coated dishes for 2 h in 1 × MBS. Caps were incubated with 50 μg/ml of transferrin-633 for 30 mins at 4°C in the dark, and then allowed to uptake transferrin-633 for 25 mins (first 5 mins at 37°C; last 20 mins at room temperature with gentle agitation). Caps were washed 5 × with cold 1 × MBS on ice, briefly spun down at 8000 *g* at 4°C, and then four caps per well were solubilized by vortexing for 15 s in 0.2 ml of 0.25% Triton X-100 in PBS. Protein was harvested by centrifuging at 15 000 *g* for 5 mins and the supernatant was analysed for fluorescence (excitation = 488; emission = 633). Protein concentration of the animal caps was determined using a BCA assay (Thermo Scientific, 23227) and fluorescent units/μg of protein was determined. For side-by-side comparison of control and experimental models, Bves MO, Bves MOR, VAMP3 MO, and VAMP3 MOR data are reported as percentage of the control (COMO).

Scratch assay

A scratch assay was performed and scored for the amount of internalized β-1-integrin, according to Proux-Gillardeaux *et al*. For scratch assays that directly compared TeNT cells and Bves118 cells, CD29 was conjugated to Alexa-564 (Molecular Probes) and conducted in triplicate.

Cell spreading assay in MDCK cells

Cell spreading was defined as the increase of cell area over time prior to polarized cell movement. One day before cell spreading analysis, cells were plated at single-cell density so that they would be contact naïve at the time of the assay. On the day of image acquisition, cells were trypsinized and plated at single-cell density on MatTek dishes (MatTek Corporation) coated with 25 μg/ml of FN (Sigma, F4759). Attached yet rounded cells were chosen 45 mins after plating and DIC images were acquired with a temperature- and CO_2-controlled WeatherStation as part of a DeltaVision platform (Precision Control). Images were obtained with an Olympus IX71 inverted microscope and a CoolSNAP-HQ2 CCD camera using the × 40 objective at intervals of 1 min for 1 h. Images were deconvoluted with the SoftWorx software. Metamorph 6.0 was used to determine cell area and construct kymographs from DIC images every tenth minute.

X. laevis embryos

Female *X. laevis* were obtained from Nasco, primed, and fertilized by standard methods (Ripley *et al*, 2006). Images of appropriately staged embryos (Nieuwkoop and Faber, 1994) were captured with Magnafire (Olympus America Diagnostics).

Microinjection and MO treatment

Embryos were microinjected with 5 nl into both cells at stage-2; embryos were injected in 5% Ficoll in 1 × Steinberg's Solution (SS), and then switched to 0.1 × SS before gastrulation. Bves MO, VAMP3 MO, or COMO were injected into sister embryos along with mGFP or mRFP (1.5 ng), as tracer, at a concentration of 20 ng (stage 35–42 analysis only) or 40 ng per embryo (Gene Tools, LLC) (Wallingford *et al*, 2000; Ripley *et al*, 2006). For transferrin assays, 100 pg of rescue RNA (described above) was co-injected along with Bves MO or VAMP3 MO. Xbves Rescue RNA has been reported previously (Ripley *et al*, 2006) and is mutated in the MO-binding sequence, thus not recognized by Bves MO. The most successful MO for knockdown of *X. laevis* VAMP3 was designed against the 5′-UTR, approximately 20 bp upstream from the ATG site: GGA CACCGGTCCGACTTTACTC (Gene Tools, LLC). Note that this sequence is perfectly conserved with *Xenpus tropicalis*, but has no conservation with rat VAMP3 (EST databases).

Scanning electron microscopy

Embryos were fixed and processed for SEM following standard methods and HM was dissected out (the overlying BCR was peeled away from this region to expose cells that are attached to FN) with eyebrow knives. SEM images were quantified as follows: cells were chosen from random fields from 10 different embryos and measured for cellular overlap and polarity using the leading edge as a reference point. Overlap was defined as the number of overlapping cell bodies or lamellipodia for each selected cell. Polarity was determined by defining the length/width axis (longest axis of the cell intersected perpendicularly by the widest part of the cell), measuring the deviation of this axis from a set point, and then averaging the standard deviations from the defined point.

X. laevis microdissections, adhesion assays, and spreading assays

X. laevis embryos were microdissected according to the procedure of Ren *et al* (2006). Explants were disassociated in Ca^{2+} Mg^{2+}-free MBS and single cells were plated in MBS on slides (for adhesion

assays; LabTek) or on MatTek dishes (for spreading assays) coated with 200 μg/ml of FN (Sigma, F4759). Explants from several embryos (control or experimental) were pooled and plated for either adhesion or spreading assays.

Adhesion assays on FN were conducted and scored as described by Ramos and DeSimone (1996). Cells were cultured for 2 h, washed three times in MBS to remove non-adhered cells, fixed in PFA overnight at 4°C, labelled with phalloidin, and imaged with a Zeiss Inverted LSM 510 confocal microscope using a $\times 40$ objective. Round cells were attached to the plate and spherical, while spread cells were elongated and had two or more lamellipodia as previously defined (Ramos and DeSimone, 1996).

For spreading analysis, time-lapse images were obtained with the DeltaVision platform. Movies of mGFP- or mRFP-labelled cells were prepared over a 35-min timeframe, with fluorescence and DIC images being collected every minute. The point of cell–matrix interaction was used as the focal point in obtaining these images. Quantification of lamellipodia and cell spreading are as follows: for at least 12 different cells, the average number of lamellipodia (defined here as 10-μm extensions devoid of yolk granules with distinct matrix attachment sites) was determined for 10 time points at 3-min intervals over the period of culture for both control and experimental groups. Metamorph 6.0 was used to analyse every third frame to determine the cell area and construct kymographs.

Supplementary data
Supplementary data are available at *The EMBO Journal* Online (http://www.embojournal.org).

Acknowledgements

We thank Dr W Trimble (University of Toronto) for the VAMP3–GFP construct, Dr E Tahinci for his instruction on microdissection, Dr J Williams for nucleofection guidance, Dr A Major for flow cytometry expertise, and the laboratory members for careful editing of the paper. We also acknowledge Dr J Roland of the Epithelial Biology Center Imaging Resource; C Alford and the Vanderbilt VA Flow Cytometry Laboratory, and Dr J Jerome and S Schaffer of the Vanderbilt Cell Imaging Shared Resource for help in image acquisition and quantification; and Dr C Cobb of the Molecular Physiology Core. This work was supported by NIH grants HL79050 and HL07411; and in part by grants from the ARC.

Author contributions: HAH, VPG, and DMB designed the research; HAH, RJR, and EEC performed the research; HAH and DMB analysed the data and wrote the paper.

Conflict of interest

The authors declare that they have no conflict of interest.

References

Andree B, Fleige A, Arnold HH, Brand T (2002) Mouse Pop1 is required for muscle regeneration in adult skeletal muscle. *Mol Cell Biol* **22:** 1504–1512

Andree B, Hillemann T, Kessler-Icekson G, Schmitt-John T, Jockusch H, Arnold HH, Brand T (2000) Isolation and characterization of the novel popeye gene family expressed in skeletal muscle and heart. *Dev Biol* **223:** 371–382

Bajno L, Peng XR, Schreiber AD, Moore HP, Trimble WS, Grinstein S (2000) Focal exocytosis of VAMP3-containing vesicles at sites of phagosome formation. *J Cell Biol* **149:** 697–706

Bhattacharya S, Stewart BA, Niemeyer BA, Burgess RW, McCabe BD, Lin P, Boulianne G, O'Kane CJ, Schwarz TL (2002) Members of the synaptobrevin/vesicle-associated membrane protein (VAMP) family in *Drosophila* are functionally interchangeable *in vivo* for neurotransmitter release and cell viability. *Proc Natl Acad Sci USA* **99:** 13867–13872

Borisovska M, Zhao Y, Tsytsyura Y, Glyvuk N, Takamori S, Matti U, Rettig J, Sudhof T, Bruns D (2005) v-SNAREs control exocytosis of vesicles from priming to fusion. *EMBO J* **24:** 2114–2126

Brand T (2005) The Popeye domain-containing gene family. *Cell Biochem Biophys* **43:** 95–103

Breton S, Nsumu NN, Galli T, Sabolic I, Smith PJ, Brown D (2000) Tetanus toxin-mediated cleavage of cellubrevin inhibits proton secretion in the male reproductive tract. *Am J Physiol Renal Physiol* **278:** F717–F725

Brunger AT (2005) Structure and function of SNARE and SNARE-interacting proteins. *Q Rev Biophys* **38:** 1–47

Bryan B, Kumar V, Stafford LJ, Cai Y, Wu G, Liu M (2004) GEFT, a Rho family guanine nucleotide exchange factor, regulates neurite outgrowth and dendritic spine formation. *J Biol Chem* **279:** 45824–45832

Bryan BA, Cai Y, Liu M (2006) The Rho-family guanine nucleotide exchange factor GEFT enhances retinoic acid- and cAMP-induced neurite outgrowth. *J Neurosci Res* **83:** 1151–1159

Bryant DM, Stow JL (2004) The ins and outs of E-cadherin trafficking. *Trends Cell Biol* **14:** 427–434

Cai H, Reinisch K, Ferro-Novick S (2007) Coats, tethers, Rabs, and SNAREs work together to mediate the intracellular destination of a transport vesicle. *Dev Cell* **12:** 671–682

Caswell P, Norman J (2008) Endocytic transport of integrins during cell migration and invasion. *Trends Cell Biol* **18:** 257–263

Caswell PT, Norman JC (2006) Integrin trafficking and the control of cell migration. *Traffic* **7:** 14–21

Davidson LA, Marsden M, Keller R, Desimone DW (2006) Integrin alpha5beta1 and fibronectin regulate polarized cell protrusions required for *Xenopus* convergence and extension. *Curr Biol* **16:** 833–844

Deak F, Shin OH, Kavalali ET, Sudhof TC (2006) Structural determinants of synaptobrevin 2 function in synaptic vesicle fusion. *J Neurosci* **26:** 6668–6676

DeMali KA, Wennerberg K, Burridge K (2003) Integrin signaling to the actin cytoskeleton. *Curr Opin Cell Biol* **15:** 572–582

Desclozeaux M, Venturato J, Wylie FG, Kay JG, Joseph SR, Le HT, Stow JL (2008) Active Rab11 and functional recycling endosome are required for E-cadherin trafficking and lumen formation during epithelial morphogenesis. *Am J Physiol Cell Physiol* **295:** C545–C556

DeSimone DW, Davidson L, Marsden M, Alfandari D (2005) The *Xenopus* embryo as a model system for studies of cell migration. *Methods Mol Biol* **294:** 235–245

Dunnwald M, Varshavsky A, Johnsson N (1999) Detection of transient *in vivo* interactions between substrate and transporter during protein translocation into the endoplasmic reticulum. *Mol Biol Cell* **10:** 329–344

Etienne-Manneville S, Hall A (2002) Rho GTPases in cell biology. *Nature* **420:** 629–635

Fackler OT, Grosse R (2008) Cell motility through plasma membrane blebbing. *J Cell Biol* **181:** 879–884

Feng Q, Hawes SE, Stern JE, Wiens L, Lu H, Dong ZM, Jordan CD, Kiviat NB, Vesselle H (2008) DNA methylation in tumor and matched normal tissues from non-small cell lung cancer patients. *Cancer Epidemiol Biomarkers Prev* **17:** 645–654

Fields IC, Shteyn E, Pypaert M, Proux-Gillardeaux V, Kang RS, Galli T, Folsch H (2007) v-SNARE cellubrevin is required for basolateral sorting of AP-1B-dependent cargo in polarized epithelial cells. *J Cell Biol* **177:** 477–488

Galli T, Chilcote T, Mundigl O, Binz T, Niemann H, De Camilli P (1994) Tetanus toxin-mediated cleavage of cellubrevin impairs exocytosis of transferrin receptor-containing vesicles in CHO cells. *J Cell Biol* **125:** 1015–1024

Grosshans BL, Ortiz D, Novick P (2006) Rabs and their effectors: achieving specificity in membrane traffic. *Proc Natl Acad Sci USA* **103:** 11821–11827

Guo X, Stafford LJ, Bryan B, Xia C, Ma W, Wu X, Liu D, Songyang Z, Liu M (2003) A Rac/Cdc42-specific exchange factor, GEFT, induces cell proliferation, transformation, and migration. *J Biol Chem* **278:** 13207–13215

Hager HA, Bader DM (2009) Bves: ten years after. *Histol Histopathol* **24:** 777–787

Hirohashi S (1998) Inactivation of the E-cadherin-mediated cell adhesion system in human cancers. *Am J Pathol* **153:** 333–339

Holly SP, Larson MK, Parise LV (2000) Multiple roles of integrins in cell motility. *Exp Cell Res* **261:** 69–74

Jahn R, Scheller RH (2006) SNAREs—engines for membrane fusion. *Nat Rev Mol Cell Biol* **7:** 631–643

Johnson KE (1976) Circus movements and blebbing locomotion in dissociated embryonic cells of an amphibian, *Xenopus laevis*. *J Cell Sci* **22:** 575–583

Johnson KE, Darribere T, Boucaut JC (1993) Mesodermal cell adhesion to fibronectin-rich fibrillar extracellular matrix is required for normal *Rana pipiens* gastrulation. *J Exp Zool* **265:** 40–53

Kawaguchi M, Hager HA, Wada A, Koyama T, Chang MS, Bader DM (2008) Identification of a novel intracellular interaction domain essential for Bves function. *PLoS ONE* **3:** e2261

Keller RE (1980) The cellular basis of epiboly: an SEM study of deep-cell rearrangement during gastrulation in *Xenopus laevis*. *J Embryol Exp Morphol* **60:** 201–234

Knight RF, Bader DM, Backstrom JR (2003) Membrane topology of Bves/Pop1A, a cell adhesion molecule that displays dynamic changes in cellular distribution during development. *J Biol Chem* **278:** 32872–32879

Kumano G, Smith WC (2002) Revisions to the *Xenopus* gastrula fate map: implications for mesoderm induction and patterning. *Dev Dyn* **225:** 409–421

Lanzetti L (2007) Actin in membrane trafficking. *Curr Opin Cell Biol* **19:** 453–458

Leabu M (2006) Membrane fusion in cells: molecular machinery and mechanisms. *J Cell Mol Med* **10:** 423–427

Lin S, Zhao D, Bownes M (2007) Blood vessel/epicardial substance (bves) expression, essential for embryonic development, is down regulated by Grk/EFGR signalling. *Int J Dev Biol* **51:** 37–44

Luftman K, Hasan N, Day P, Hardee D, Hu C (2009) Silencing of VAMP3 inhibits cell migration and integrin-mediated adhesion. *Biochem Biophys Res Commun* **380:** 65–70

Marsden M, DeSimone DW (2001) Regulation of cell polarity, radial intercalation and epiboly in *Xenopus*: novel roles for integrin and fibronectin. *Development* **128:** 3635–3647

Marsden M, DeSimone DW (2003) Integrin–ECM interactions regulate cadherin-dependent cell adhesion and are required for convergent extension in *Xenopus*. *Curr Biol* **13:** 1182–1191

McCarthy M (2006) Allen brain Atlas maps 21 000 genes of the mouse brain. *Lancet Neurol* **5:** 907–908

McMahon HT, Ushkaryov YA, Edelmann L, Link E, Binz T, Niemann H, Jahn R, Sudhof TC (1993) Cellubrevin is a ubiquitous tetanus-toxin substrate homologous to a putative synaptic vesicle fusion protein. *Nature* **364:** 346–349

Mellman I, Nelson WJ (2008) Coordinated protein sorting, targeting and distribution in polarized cells. *Nat Rev Mol Cell Biol* **9:** 833–845

Na J, Marsden M, DeSimone DW (2003) Differential regulation of cell adhesive functions by integrin alpha subunit cytoplasmic tails *in vivo*. *J Cell Sci* **116:** 2333–2343

Nieuwkoop PD, Faber J (1994) *Normal Table of Xenopus laevis (Daudin): a Systematical and Chronological Survey of the Development from the Fertilized Egg Till the End of Metamorphosis*. New York: Garland Pub

Osler ME, Bader DM (2004) Bves expression during avian embryogenesis. *Dev Dyn* **229:** 658–667

Osler ME, Chang MS, Bader DM (2005) Bves modulates epithelial integrity through an interaction at the tight junction. *J Cell Sci* **118:** 4667–4678

Osler ME, Smith TK, Bader DM (2006) Bves, a member of the Popeye domain-containing gene family. *Dev Dyn* **235:** 586–593

Pfeffer SR (2007) Unsolved mysteries in membrane traffic. *Annu Rev Biochem* **76:** 629–645

Polgar J, Chung SH, Reed GL (2002) Vesicle-associated membrane protein 3 (VAMP-3) and VAMP-8 are present in human platelets and are required for granule secretion. *Blood* **100:** 1081–1083

Proux-Gillardeaux V, Gavard J, Irinopoulou T, Mege RM, Galli T (2005) Tetanus neurotoxin-mediated cleavage of cellubrevin impairs epithelial cell migration and integrin-dependent cell adhesion. *Proc Natl Acad Sci USA* **102:** 6362–6367

Ramos JW, DeSimone DW (1996) *Xenopus* embryonic cell adhesion to fibronectin: position-specific activation of RGD/synergy site-dependent migratory behavior at gastrulation. *J Cell Biol* **134:** 227–240

Ramos JW, Whittaker CA, DeSimone DW (1996) Integrin-dependent adhesive activity is spatially controlled by inductive signals at gastrulation. *Development* **122:** 2873–2883

Ren R, Nagel M, Tahinci E, Winklbauer R, Symes K (2006) Migrating anterior mesoderm cells and intercalating trunk mesoderm cells have distinct responses to Rho and Rac during *Xenopus* gastrulation. *Dev Dyn* **235:** 1090–1099

Ridley AJ (2001) Rho proteins: linking signaling with membrane trafficking. *Traffic* **2:** 303–310

Ripley AN, Chang MS, Bader DM (2004) Bves is expressed in the epithelial components of the retina, lens, and cornea. *Invest Ophthalmol Vis Sci* **45:** 2475–2483

Ripley AN, Osler ME, Wright CV, Bader D (2006) Xbves is a regulator of epithelial movement during early *Xenopus laevis* development. *Proc Natl Acad Sci USA* **103:** 614–619

Schwartz MA, Shattil SJ (2000) Signaling networks linking integrins and rho family GTPases. *Trends Biochem Sci* **25:** 388–391

Segev N (2001) Ypt/rab gtpases: regulators of protein trafficking. *Sci STKE* **2001:** RE11

Selchow A, Winklbauer R (1997) Structure and cytoskeletal organization of migratory mesoderm cells from the *Xenopus* gastrula. *Cell Motil Cytoskeleton* **36:** 12–29

Shook D, Keller R (2003) Mechanisms, mechanics and function of epithelial–mesenchymal transitions in early development. *Mech Dev* **120:** 1351–1383

Skalski M, Coppolino MG (2005) SNARE-mediated trafficking of alpha5beta1 integrin is required for spreading in CHO cells. *Biochem Biophys Res Commun* **335:** 1199–1210

Smith JC, Symes K, Hynes RO, DeSimone D (1990) Mesoderm induction and the control of gastrulation in *Xenopus laevis*: the roles of fibronectin and integrins. *Development* **108:** 229–238

Smith TK, Bader DM (2006) Characterization of Bves expression during mouse development using newly generated immunoreagents. *Dev Dyn* **235:** 1701–1708

Smith TK, Hager HA, Francis R, Kilkenny DM, Lo CW, Bader DM (2008) Bves directly interacts with GEFT, and controls cell shape and movement through regulation of Rac1/Cdc42 activity. *Proc Natl Acad Sci USA* **105:** 8298–8303

Symons M, Rusk N (2003) Control of vesicular trafficking by Rho GTPases. *Curr Biol* **13:** R409–R418

Tajika Y, Sato M, Murakami T, Takata K, Yorifuji H (2007) VAMP2 is expressed in muscle satellite cells and upregulated during muscle regeneration. *Cell Tissue Res* **328:** 573–581

Tayeb MA, Skalski M, Cha MC, Kean MJ, Scaife M, Coppolino MG (2005) Inhibition of SNARE-mediated membrane traffic impairs cell migration. *Exp Cell Res* **305:** 63–73

Torlopp A, Breher SS, Schluter J, Brand T (2006) Comparative analysis of mRNA and protein expression of Popdc1 (Bves) during early development in the chick embryo. *Dev Dyn* **235:** 691–700

Vasavada TK, DiAngelo JR, Duncan MK (2004) Developmental expression of Pop1/Bves. *J Histochem Cytochem* **52:** 371–377

Wada AM, Reese DE, Bader DM (2001) Bves: prototype of a new class of cell adhesion molecules expressed during coronary artery development. *Development* **128:** 2085–2093

Wallingford JB, Rowning BA, Vogeli KM, Rothbacher U, Fraser SE, Harland RM (2000) Dishevelled controls cell polarity during *Xenopus* gastrulation. *Nature* **405:** 81–85

Winklbauer R, Nagel M (1991) Directional mesoderm cell migration in the *Xenopus* gastrula. *Dev Biol* **148:** 573–589

Yap AS, Crampton MS, Hardin J (2007) Making and breaking contacts: the cellular biology of cadherin regulation. *Curr Opin Cell Biol* **19:** 508–514